

Electronic Supplementary Information

Ion Current Behaviors of Mesoporous Zeolite/Polymer Composite Nanochannels Prepared by Water-assisted Self-assembly

Wenjuan Zhang,^a Zheyi Meng, Jin Zhai^{a,*}, Liping Heng^b

a. Key Laboratory of Bio-Inspired Smart Interfacial Science and Technology of Ministry of Education, School of Chemistry and Environment, Beihang University, Beijing 100191, P. R. China

b. Institute of Chemistry, Chinese Academy of Sciences
Beijing 100190, P. R. China

Email: zhaijin@buaa.edu.cn

Experimental

1. Materials

PI (Polyimide resin) was purchased from Alfa Aesar Chemical Co., Ltd.

MCM-41 was purchased from Nanjing XFNANO Materials TECH Co.,Ltd.

Chloroform, potassium chloride (KCl), sodium chloride (NaCl) and lithium chloride (LiCl)

All reagents above were used as received and were analytical graded.

2. Preparation of the composite nanochannel membrane

Asymmetry mesoporous zeolite/polymer composite nanochannels (MZPCN) based on MCM-41 and polyimide (PI) were obtained by water-assisted self-assembly. In brief, a mount of MCM-41 powder was dispersed in Chloroform solvent by ultrasonic dispersion, and then PI was added to the mix. After complete dissolution, the resulting solution was cast onto a smooth, clean glass plate, and the desired thickness was produced using a doctor blade. The solvent was evaporated in a wet atmosphere (relative humidity: $80\% \pm 5\%$ and room temperature: $20 \pm 3^\circ\text{C}$) followed by drying under this atmosphere to form nanochannel-1 (porous film). For comparison purposes, nanochannel-2 (smooth film), forming in a dry atmosphere (relative humidity: under

20%), were also prepared.

3. Characterization of the composite nanochannel membranes

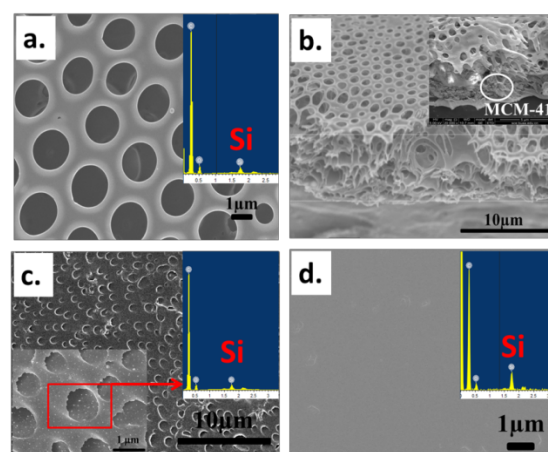


Fig. S1 (a) SEM observations and EDS results (inset) of the channel-1 membrane surface. (b) Cross-sectional SEM image of the channel-1 membrane. (c) SEM images and EDS results (inset) of the nanochannel-1 membrane back. (d) SEM observations and EDS results (inset) of the channel-2 membrane surface.

Fig. S1(a) depicts the typical SEM morphologies of channel-1 membrane. The side of membrane with large pore diameter is defined to be base side, which has an average pore diameter of 800~1800 nm. The thickness of the nanochannel-1 membrane is determined to be ~10μm based on the cross-sectional images (Fig. S1(b)). In Fig. S1(c), SEM of the nanochannel-1 membrane back, there are no pvious pores, but we can see the existence of mesoporous structure. SEM and EDS confirm that mesoporous silica (MCM-41) is present in the membranes. Combined with SEM images of the surface, back and the cross-section of the membrane, the asymmetric structure can be supported.

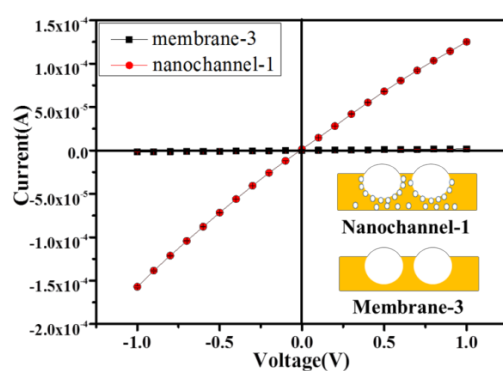


Fig. S2. I-V curves of nanochannel-1 and membrane-3 record under symmetric electrolyte conditions at 10 mM KCl. Illustration of nanochannel-1 and membrane-3 (inset).

In order to further clarify, we fabricated the membrane-3 based polyimide (PI) without MCM-41 by water-assisted self-assembly. We investigated the current–voltage (I-V) characteristics of nanochannel-1 and membrane-3(Fig. S2). The nanochannel-1 showed a high conductivity and high ion current compared with membrane-3, which revealed the role of molecular sieves. The result further confirmed the role of molecular sieves in the asymmetric structure of the nanochannel-1.

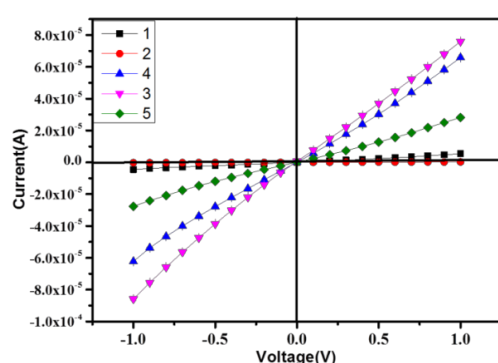


Fig. S3. I-V curves of membranes fabricated under different humidity at 10 mM KCl.
(Relative humidity: 1,35%-40%; 2,50%-60%; 3,75%-80%; 4,80%-85%. 5,above 90%.)

We fabricated membranes in various relative humidity. At the same time, ion-transport behaviors of nanochannels have been discussed(Fig. S3). The membrane made under the humidity below 60%, shows a low ion current. And, the membrane , fabricated under humidity of 80% \pm 5%, shows a higher ion current. However, when the membrane fabricated under the humidity of above 90% , the ion current reduced. In simple terms, the ion current increases with humidity at first and then decreases. Thus, we got the optimal humidity conditions: 80 \pm 5%.

4. The molecular sieves were fully characterized by means of N₂-adsorption–desorption, transmission electron microscopy (TEM).

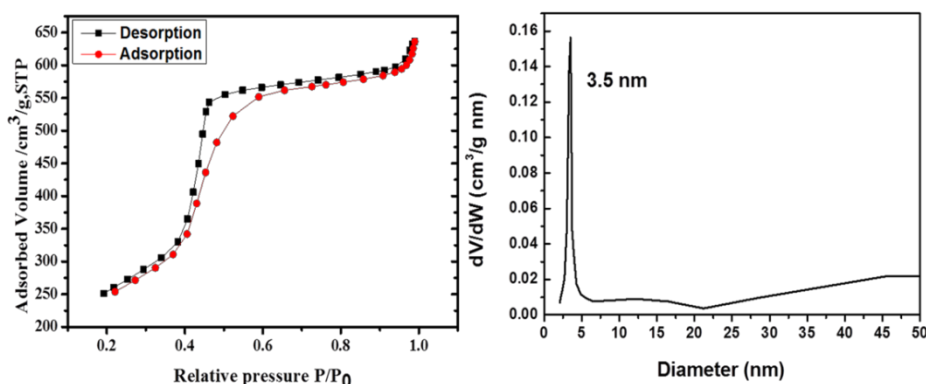


Fig. S4 Sorption isotherm (left) and pore size distribution (BJH plot) (right) of MCM-41

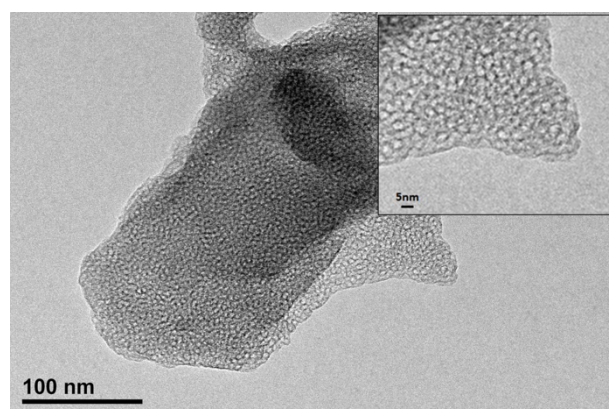


Fig. S5 TEM images showing the mesoporous structure of MCM-41

According to the TEM analysis (Fig. S5) and BET measurements (Fig. S4), the mesoporous material had a total surface area of up to $1074 \text{ m}^2 \cdot \text{g}^{-1}$, exhibiting a characteristic pore size distribution with a sharp peak around 3.5 nm. The experimental value for MCM-41 is in accordance with our expectations. These results can be qualitatively summarized in Table. S1.

Table. S1 The characteristics of MCM-41

type of material	BET surface [$\text{m}^2 \cdot \text{g}^{-1}$]	average pore diameter [nm]
MCM-41	1074	3.5

5. The diffusion coefficient of cation (D_+) and anion (D_-) in different electrolytes.

Table. S2 The diffusion coefficient of cation (D_+) and anion (D_-) in different electrolytes.¹

	$D_+ (10^{-5} \text{ cm}^2 \cdot \text{s}^{-1})$	$D_- (10^{-5} \text{ cm}^2 \cdot \text{s}^{-1})$	Ratio(D_+/D_-)
KCl	1.957	2.032	0.96
NaCl	1.334	2.032	0.65
LiCl	1.029	2.032	0.50

6. Ion current measurement

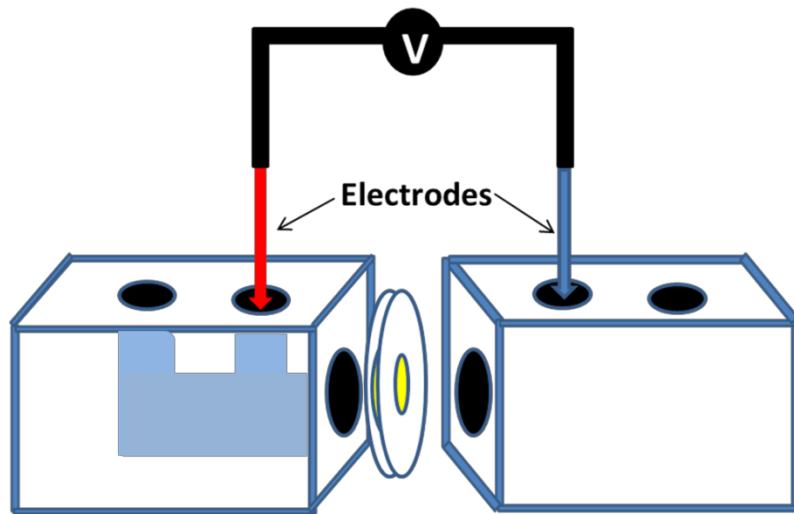


Fig. S6 The experimental cell used in the ion current measurement experiment. The anode (red arrow) faced the base of the nanochannel.

The ionic transport properties of the nanochannel were studied by measuring ionic current through the nanochannel. Ionic current was measured by a Keithley 6487 picoammeter (Keithley Instruments, Cleveland, OH). The membrane was mounted between two chambers of the etching cell. Ag/AgCl electrodes were used to apply a transmembrane potential across the film. A scanning voltage varied from -1 V to +1 V at a scanning rate of 40 s. Two silver/silver chloride electrodes were immersed on the tip side and the base side of the nanochannel, respectively.

References:

1. L. Cao, W. Guo, W. Ma, L. Wang, F. Xia, S. Wang, Y. Wang, L. Jiang and D. Zhu, *Energy & Environmental Science*, 2011, **4**, 2259.